The Q267E mutation in the sodium/iodide symporter (NIS) causes congenital iodide transport defect (ITD) by decreasing the NIS turnover number

Antonio De la Vieja, Christopher S. Ginter and Nancy Carrasco*

Department of Molecular Pharmacology, Albert Einstein College of Medicine, 1300 Morris Park Avenue, Bronx, NY 10461, USA
*Author for correspondence (e-mail: carrasco@aecom.yu.edu)

Accepted 19 September 2003
Journal of Cell Science 117, 677-687 Published by The Company of Biologists 2004
doi:10.1242/jcs.00898

Summary

The Na^+/I^- symporter (NIS) is a key plasma membrane glycoprotein that mediates active iodide (I^-) transport in the thyroid and other tissues. Since isolation of the cDNA encoding NIS (G. Dai, O. Levy, and N. Carrasco (1996) *Nature* 379, 458-460), ten mutations in NIS have been identified as causes of congenital iodide transport defect (ITD). Two of these mutations (T354P and G395R) have been thoroughly characterized at the molecular level. Both mutant NIS proteins are inactive but normally expressed and correctly targeted to the plasma membrane. The hydroxyl group at the β-carbon of residue 354 is essential for NIS function, whereas the presence of a charged or large side-chain at position 395 interferes with NIS function. We report the extensive molecular analysis of the Q267E mutation in COS-7 cells transfected with rat or human Q267E NIS cDNA constructs. We used site-directed mutagenesis to engineer various residue substitutions into position 267. In contrast to previous suggestions that Q267E NIS was inactive, possibly because of a trafficking defect, we conclusively show that Q267E NIS is modestly active and properly targeted to the plasma membrane. Q267E NIS exhibited lower V_{max} values for I^- than wild-type NIS, suggesting that the decreased level of activity of Q267E NIS is due to a lower catalytic rate. That Q267E NIS retains even partial activity sets this ITD-causing mutant apart from T354P and G395R NIS. The presence of charged residues (of any polarity) other than Glu at position 267 rendered NIS inactive without affecting its expression or targeting, but substitution with neutral residues at this position was compatible with partial activity.

Key words: NIS (sodium/iodide symporter), ITD (iodide transport defect), Thyroid, Membrane proteins

Introduction

Iodide (I^-) is an essential constituent of the thyroid hormones T_3 and T_4 (triiodothyronine and thyroxine, or tetraiodothyronine, respectively). These hormones play a central role in the intermediary metabolism of virtually all tissues and are vital for the development of the central nervous system in the fetus and the newborn. The thyroid has a highly specialized plasma membrane glycoprotein, the sodium/iodide symporter (NIS), that mediates the active transport of I^- from the bloodstream into the thyroid follicular cells. The presence of NIS in the thyroid may be an apparent adaptation to overcome the scarcity of I^- in the environment (Stephenson et al., 2000). NIS couples the inward transport of Na^+, which occurs in favor of its electrochemical gradient, to the simultaneous inward translocation of I^- against its electrochemical gradient. NIS activity is electrogenic: two Na^+ ions are translocated per I^- ion (Dai et al., 1996; Eskandari et al., 1997). NIS-mediated active I^- transport is driven by the Na^+ gradient generated by the Na^+/K^+-ATPase. NIS concentrates I^- in thyroid cells by a factor of 20-40 with respect to the blood under physiological conditions (Carrasco, 1993).

The rat and human NIS cDNAs encode a 618 and a 643 amino acid protein, respectively (Dai et al., 1996; Smanik et al., 1996; Smanik et al., 1997). Human NIS has an 84% amino acid identity and a 93% similarity to rat NIS. The current NIS secondary structure model (Fig. 1A) depicts NIS as a protein with 13 transmembrane segments, the amino terminus facing the extracellular milieu, and the carboxyl terminus facing the cytosol; the location of both termini has been confirmed experimentally (Levy et al., 1997; Levy et al., 1998b). Several extensive reviews on recent NIS research have been published (Levy et al., 1998a; De la Vieja et al., 2000; Spitzweg et al., 2002; Chung, 2002; Dohan et al., 2003).

Before isolation of the NIS cDNA, several cases of congenital hypothyroidism due to an I^- transport defect (ITD) (OMIM 274400; online, Mendelian Inheritance in Man, http://www.ncbi.nlm.nih.gov/OMIM) were reported (Wolff, 1983). ITD is an uncommon condition caused by NIS mutations with an autosomal recessive inheritance pattern. The isolation of the NIS cDNA made it possible to address the molecular basis of ITD.

The general clinical picture of ITD consists of a variable degree of hypothyroidism; large or small goiter; reduced or absent thyroid uptake of radioiodide or pertechnetate, as determined by scintigraphy; and a low I^- saliva to plasma (S/P) ratio (normal >20). Ten NIS ITD mutations have been identified so far: V59E, G93R, Q267E, C272X, G395R, T354P, frame-shift 515X, Y531X, G543E and ΔM143-Q323 (Fujiwara et al., 1997; Matsuda and Kosugi, 1997; Fujiwara et al., 1998; Kosugi et al., 1998a; Kosugi et al., 1998b; Pohlenz et al., 1997;

Pohlenz et al., 1998; Kosugi et al., 1999; Kosugi et al., 2002; Levy et al., 1998c) (Fig. 1A). They are either nonsense, alternative splicing, frame-shift, deletion or missense mutations of the NIS gene. Although the clinical picture and genetic alterations of patients with these defects are well described, the molecular mechanisms underlying the effects of these mutations have yet to be elucidated, with the exception of T354P (Levy et al., 1998c) and G395R (Dohan et al., 2002).

The Q267E substitution was detected in a patient who carried a compound heterozygous mutation (Pohlenz et al., 1998). From the maternal allele, the patient inherited a substitution of cytosine by guanidine at nucleotide 1940 at exon 13. From the paternal allele, the patient inherited a substitution of cytosine by guanidine at nucleotide 1146 (exon 6) that resulted in a Gln-for-Glu amino acid replacement (Q267E). This mutation is located in the intracellular loop between transmembrane segments VII and VIII (Fig. 1A). Although the patient carries a compound heterozygous mutation, the final functional result is equivalent to being homozygous for the Q267E mutation. Pohlenz et al. reported in 1998 that COS-7 cells transfected with the Q267E NIS cDNA did not exhibit I^- transport activity (Pohlenz et al., 1998). Subsequently, Pohlenz et al. (Pohlenz et al., 2000) detected no Q267E NIS by flow cytometry analysis in the plasma membrane of Q267E-NIS-expressing COS-7 cells, a finding they attributed to impaired trafficking caused by the mutation.

We have carried out a thorough molecular analysis of the Q267E NIS substitution. Using a wide variety of approaches (flow cytometry, immunoblot analysis, immunofluorescence and biotinylation), we found, surprisingly, that Q267E NIS is correctly targeted to the plasma membrane. Furthermore, initial-rate and steady-state analysis of I^- transport activity showed that COS-7 cells transfected with Q267E NIS do actively concentrate I^-, if only by a factor of ~2.5. By comparison, wild-type (WT) NIS concentrates I^- >30 fold. Our results demonstrate that the Q267E mutation leads to a marked decrease, but not a total absence, of I^- transport activity. This decrease, in turn, is due to a pronounced lowering of the NIS V_{max} for I^-, not to a trafficking defect.

Materials and Methods

Site-directed mutagenesis

Individual mutagenic oligonucleotides were generated to make the following substitutions at the Q267 position. rQ267A: GCCCAGGTAGCACGCT ATGTGG; rQ267P: GCCCAGGTACCG-CGCTATGTGG; rQ267N: GCCCAGGTAAACCGCTATGTGG; rQ267W: GCCCAGGTATGGCGCTATGTGG; rQ267D: GCCCA-GGTAGACCGCTATGTGG; rQ267E: GCCCAGGTAGAACGCTA-TGTGG; rQ267K: GCCCAGGTAAAGCGCTATGTGG; rQ267R: GCCCAGGTACGCCGCTATGTGG. The initial PCR extensions were performed using reverse primers complementary to the 3′ end. These fragments were gel purified and used for a second round PCR extension with primers complementary to the 5′ end. Fragments with the mutant sequences were obtained by digestion of the final PCR products with the appropriate unique restriction enzymes that would yield the smallest mutant fragments. These fragments were ligated into WT NIS cDNA (pSVSport-rNIS) and the mutant inserts were sequenced past their respective cloning sites.

The pSVSport-flag-rNIS WT cDNA (Levy et al., 1998b) was subcloned into a pCDNA3.1- vector (Invitrogen) by *Eco*RI/*Hin*dIII restriction sites to insert the flag sequence at the N terminus of the protein. pSVSport-rQ267E was subcloned into pcDNA3.1-flag-rNIS by *Blp*I/*Hin*dIII restriction sites to obtain pcDNA3.1-flag-rQ267E cDNA. WT hNIS cDNA inserted into the pcDNA3.1- vector by *Xba*I/*Hin*dIII restriction sites (pcDNA3.1-hNIS) was kindly provided by BRAHMS Diagnostica (Germany). hQ267E NIS cDNA (pcDNA3.1-hQ267E) was kindly provided by Dr Samuel Refetoff (University of Chicago, Chicago, Illinois).

Transient transfection

COS-7 cells were cultured and transfected as previously reported (Levy et al., 1998b). Briefly, COS-7 or HEK293 cells were transfected by the DEAE-Dextran method with 1 μg/ml rNIS or rat mutant cDNAs in pSV.SPORT (Gibco-BRL), and hNIS or human mutant in pcDNA3.1(–). After 2 days they were assayed for I^- uptake, and analyzed by immunoblotting, immunofluorescence and/or flow cytometry.

Membrane preparation

Membrane fractions were prepared from transfected cells as described previously (Levy et al., 1997).

Transport

Cells transiently transfected with WT or mutant NIS cDNA were assayed for I^- transport under steady-state conditions as described previously (Weiss et al., 1984; Levy et al., 1998b). For I^--dependent kinetic analysis, cells were incubated with the indicated concentrations of I^- (2.5-200 μM) and 140 mM NaCl for 4 minutes. For Na^+ dependence of I^- uptake, cells were incubated with the indicated concentration of Na^+ (0-200 mM) and 20 μM I^- for 4 minutes; isotonicity was maintained constant with choline chloride. Results are the average of at least five different experiments performed in triplicate or sextuplicate.

Initial-rate data were analyzed by nonlinear regression using the following equation for I^--dependent I^- uptake: $v([I^-])=(V_{max}*[I^-])/(K_m+[I^-])+0.037*[I^-]+0.171$. The terms $0.037*[I^-]+0.171$ correspond to background adjusted by least squares of the data obtained with non-transfected cells. In the Na^+-dependent I^- uptake analysis, data were analyzed using the equation: $v([Na^+])=(V_{max}*[Na^+]^2)/(K_m+[Na^+]^2)-0.001*[Na^+]+0.87$. The terms $–0.001*[I^-]+0.87$ correspond to the background adjusted by linear regression analysis obtained with non-transfected cells. Data were fitted by nonlinear least squares using the Marquard-Levenberg algorithm (Press et al., 1986).

Statistical analysis

Data were analyzed with GraphPad Prism (Intuitive software for science, San Diego, CA) and Gnuplot (www.gnuplot.info). I^- uptake values are the mean±s.d. Statistical significance was determined by *t*-test analysis using two-tailed *P* values, and differences were considered significant at $P<0.05$. K_m and V_{max} values are the average of at least five experiments and are expressed as mean±s.e.m.

Antibodies

Anti-Ct-rNIS: affinity-purified site-directed polyclonal antibody was used at a final concentration of 2 nM in immunoblot, flow cytometry and immunofluorescence analyses. This antibody was generated against the last 16 amino acids of rat NIS (Levy et al., 1997).

Anti-Ct-hNIS: affinity-purified site-directed polyclonal antibody was used at a final concentration of 4 nM in immunoblot, flow cytometry and immunofluorescence analyses. This antibody was generated against the last 13 amino acids of human NIS (Tazebay et al., 2000).

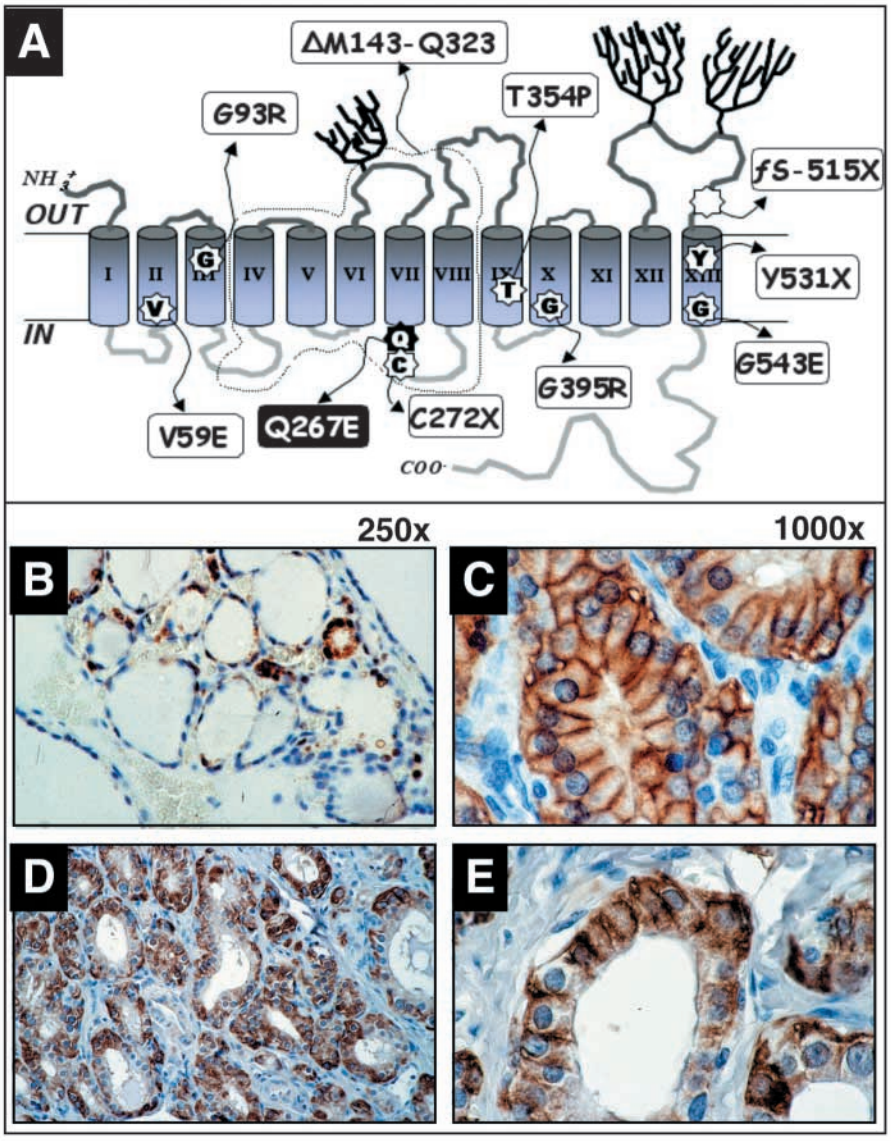

Fig. 1. Human NIS (hNIS) secondary structure model and immunohistochemistry of thyroid tissue from the Q267E NIS patient. (A) Current WT hNIS 13-transmembrane-segment secondary structure model; ITD-causing mutations are shown in rectangles by the WT residue involved, indicating its position and the substituted residue. The single-letter amino acid code is used. X, stop codon; fS, frame shift; Δ, deletion. (B-E) NIS expression was analyzed in paraffin-embedded sections of thyroid by immunohistochemistry using anti-carboxyl terminus hNIS Ab. (B) Normal thyroid staining. (C) Thyroid from a patient with Graves' disease and (D,E) thyroid from a patient with the Q267E NIS mutation (kindly provided by Dr Refetoff, Chicago University). Pronounced NIS protein staining was observed in both these cases. No immunoreactivity was detected in the presence of the C-terminus synthetic peptide (not shown). Magnifications: B,D, 250×; E,C, 1000×.

Anti-hNIS VJ1: monoclonal antibody that recognizes the last two extracellular segments of human NIS protein (kindly provided by Dr S. Costagliola, Institute of Interdisciplinary Research, Free University of Brussels, Brussels, Belgium) was used at a 1:50 dilution in flow cytometry and immunofluorescence analyses (Pohlenz et al., 2000). Anti-tubulin (Sigma) and anti-Na^+/K^+-ATPase alpha Abs (Affinity BioReagents) were used following the manufacturers' instructions.

Immunoblotting

SDS-9%PAGE, electroblotting to nitrocellulose, and probing with the corresponding Abs were performed as described previously (Levy et al., 1997).

Flow cytometry

Cells in suspension were stained using indirect immunofluorescence procedures (Jocobberger et al., 1986; Jocobberger, 1991). All procedures were carried out at 4°C. The fluorescence of 10,000 cells/tube was assayed by a FACS scan flow cytometer (Beckton Dickinson and Co.).

Immunofluorescence

Immunofluorescence was carried out as described previously (Levy et al., 1997). Confocal images were generated on a BioRad Radiance 2000 scanning laser confocal microscope. Confocal xz sections were generated using a 0.2 μm motor step.

Immunohistochemistry

Immunohistochemistry experiments were performed as described previously (Dohan et al., 2001).

Biotinylation

Cell surface proteins were labeled by two different methods. First, cells were labeled with the membrane-impermeable biotinylation reagent Sulfo-NHS-SS-biotin (Pierce Chemical Co.), as described by Chen et al. (Chen et al., 1998), and the final immunoblots were probed with anti-NIS Ab. Second, cell surface proteins were labeled with the membrane-impermeable biotinylation reagent Sulfo-NHS-LC-biotin (Pierce Chemical Co.), then immnunoprecipitated with anti-NIS Ab (Levy et al., 1997), and the immunoblots were probed with streptavidin-HRP (1:500; Amersham).

Results

NIS is overexpressed in thyroid sections from a patient with the Q267E NIS mutation

Using a polyclonal anti-carboxyl-terminus hNIS Ab, we analyzed, by immunohistochemistry, paraffin-embedded sections (kindly provided by Dr Refetoff, Chicago University) from the thyroid of a patient with the Q267E NIS mutation (Pohlenz et al., 1998) and compared them to control normal thyroid sections (Fig. 1B-E). Consistent with previous observations (Castro et al., 1999; Dohan et al., 2001), modest NIS staining was evident in the normal thyroid only in some

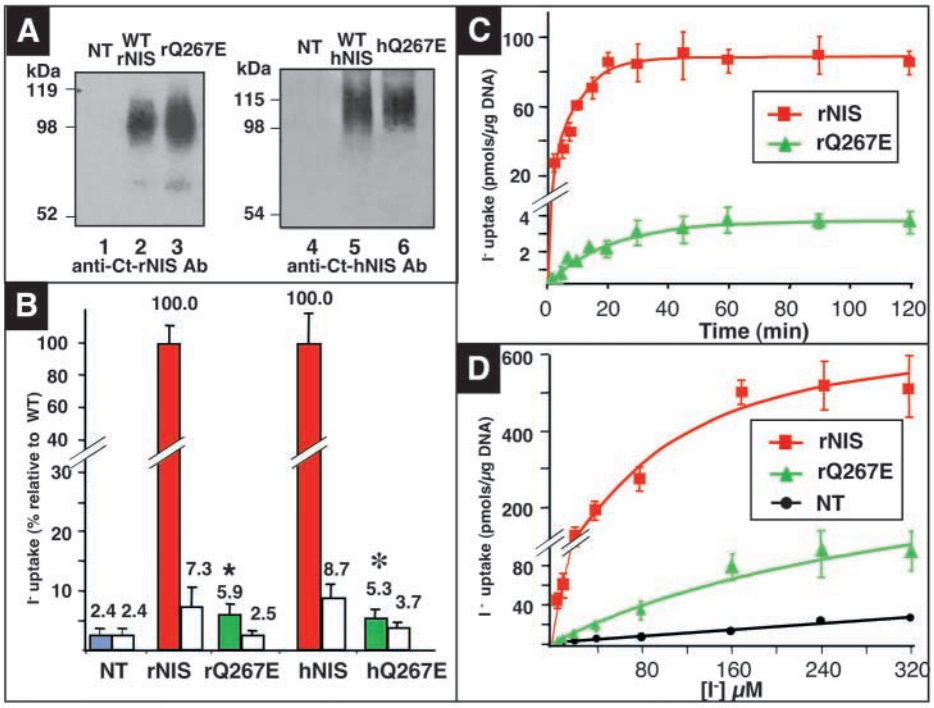

Fig. 2. Characterization of expression and activity of Q267E NIS in transfected COS-7 cells. (A) Immunoblot analysis. Membrane fractions (20 μg) were isolated from non-transfected COS-7 cells (NT) (lanes 1 and 4) or from COS-7 cells transfected either with WT rNIS (lane 2), rQ267E NIS (lane 3), WT hNIS (lane 5) or hQ267E NIS (lane 6). Membrane fractions were then electrophoresed, electrotransferred and immunoblotted with either 2 nM anti-Ct-rNIS Ab (lanes 1-3) or 4 nM anti-Ct-hNIS Ab (lanes 4-6). This is a representative immunoblot. Protein loading was standardized with anti-tubulin Ab (not shown). Expression of both NIS and tubulin was quantified in five different experiments. No statistically significant difference was found in the NIS/tubulin expression ratio of Q267E NIS when compared to WT NIS. (B) I^- transport. Assays were performed in the presence of 20 μM I^-/140 mM Na^+ (colored bars) or 20 μM I^-/140 mM Na^+ plus 80 μM perchlorate (white bars). Results are expressed as the percentage I^- uptake with respect to WT NIS. Values represent the average of at least five different experiments; in each experiment, activity was analyzed in triplicate or sextuplicate. (C) Time-course of I^- uptake in cells transfected with either WT rNIS (red squares) or rQ267E NIS (green triangles). Cells were incubated with 20 μM I^-/140 mM Na^+ for the indicated times. Values obtained with non-transfected cells were subtracted. (D) Effect of increasing concentrations of I^- on I^- uptake. COS-7 cells not transfected (black circles) or transfected with either WT rNIS (red squares) or rQ267E NIS (green triangles) were assayed at steady-state (60 minutes) in the presence of the indicated I^- concentrations. I^- uptake values are the mean±s.d. Statistical significance of the data was calculated by *t*-test analysis using two-tailed *P* values. **P*<0.05. Y-axes have been split into two scales (B–D).

cells (Fig. 1B). Thyroid sections from the patient bearing the Q267E NIS mutation had much more pronounced NIS staining, which was present both intracellularly and at the plasma membrane (Fig. 1D,E), in contrast to the pattern observed in thyroid sections from patients with Graves' disease, where plasma membrane staining was predominant (Fig. 1C). No immunoreactivity was detected in the presence of the C-terminus synthetic peptide (not shown).

The Q267E NIS mutant protein is normally expressed and exhibits modest activity in COS-7 cells

To investigate the expression and activity of Q267E NIS, we transfected rat or human Q267E NIS cDNA constructs, as well as control WT NIS cDNA, into COS-7 cells. NIS protein expression, as assessed by immunoblot analysis of membrane fractions, was similar in all transfected cells (Fig. 2A). hNIS (643 amino acids, see right panel) migrates slightly slower than rNIS (618 amino acids, left panel); both proteins are highly glycosylated. We then assayed cells for Na^+-dependent, perchlorate-inhibitable I^- transport at an external concentration of 20 μM I^- (Fig. 2B). I^- accumulation under steady-state conditions was ~2.5 times higher in Q267E-NIS-expressing cells (green bars) than in non-transfected cells (blue bar), although it was still markedly lower than in cells expressing WT NIS (red bars). This threefold rise in I^- transport activity observed in Q267E-NIS-expressing cells relative to non-transfected cells was statistically significant (Fig. 2B). The time course of transport obtained in all cells revealed that I^- accumulation takes longer to reach a plateau in Q267E-NIS- (60 minutes) than in WT-NIS-expressing cells (20 minutes) (Fig. 2C). Steady-state measurements at different I^- concentrations (Fig. 2D) showed that the difference in accumulation between cells expressing WT NIS and Q267E NIS decreases at higher substrate concentrations. The observation of NIS activity in Q267E-NIS-expressing cells demonstrates that at least some Q267E NIS is targeted to the plasma membrane, the only site where the driving force for NIS (i.e., the Na^+ gradient generated by the Na^+/K^+ ATPase) is present.

Targeting of Q267E NIS to the plasma membrane is indistinguishable from that of WT NIS

Given the report by Pohlenz et al. (Pohlenz et al., 2000) that trafficking of Q267E NIS to the cell surface was impaired, a conclusion that conflicts with the above findings, we thoroughly examined the targeting of Q267E NIS to the plasma membrane by cytometric analysis, surface biotinylation and confocal immunofluorescence (Figs 3-6). Our flow cytometry showed that, consistently with our I^- transport findings, Q267E NIS was properly targeted to the plasma membrane, in a fashion that was indistinguishable from WT NIS targeting (Fig. 3). When flow cytometry was monitored with an Ab directed against the NIS carboxyl terminus, which is an intracellularly oriented epitope, flow cytometry was only positive in permeabilized cells, where the Ab had access to the epitope (Fig. 3A,B). Moreover, flow cytometry of Q267E NIS was also

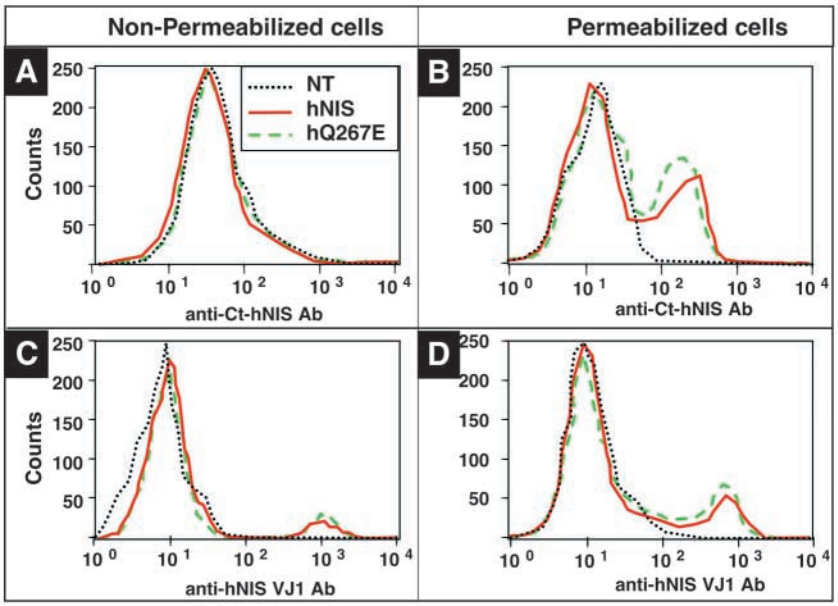

Fig. 3. Flow cytometry analysis of Q267E NIS. Non-permeabilized (A,C) or permeabilized (B,D) COS-7 cells not-transfected (black dotted line) transfected with WT hNIS (red line) or hQ267E NIS (green line) were incubated with 4 nM anti-Ct-hNIS Ab (A,B) or with a 1:50 dilution of anti-hNIS VJ1 Ab (C,D), followed by incubation with fluorescein-conjugated goat anti-rabbit Ab (A,B) or fluorescein-conjugated anti-mouse Ab (C,D). Aliquots containing 2×10^6 cells were subjected to flow cytometry.

positive in both non-permeabilized and permeabilized cells when using anti-hNIS VJ1 (Fig. 3C,D), an anti-NIS Ab directed against an extracellularly facing yet unknown epitope (Pohlenz et al., 2000). The fluorescence shift in the cells expressing Q267E NIS was virtually identical to that of WT NIS (Fig. 3B-D).

Surface biotinylation analysis was performed with the amino-specific and membrane-impermeable reagent Sulfo-NHS-SS-biotin. The entire biotinylated fraction was isolated with streptavidin-coated beads and immunoblotted with anti-NIS Abs. The observed levels of Q267E NIS at the plasma membrane were similar to those of WT NIS (Fig. 4A,D). The absence of staining on the immunoblot when the control anti-tubulin Ab was used confirmed that Sulfo-NHS-SS-biotin did not cross the plasma membrane (data not shown). Nitrocellulose membranes were stripped and reprobed with anti-Na^+/K^+-ATPase alpha subunit Ab (data not shown). Both protein bands were quantified, revealing no statistically significant difference in the NIS/ATPase-alpha-subunit expression ratio of Q267E NIS as compared to WT NIS. To rule out the unlikely possibility that NIS itself was not biotinylated directly but, instead, was precipitated with avidine as a result of NIS interaction(s) with other membrane protein(s) that were biotinylated, we used an alternative method: we precipitated the biotinylated fraction with anti-Ct-rNIS (Fig. 4B) or anti-Ct-hNIS (Fig. 4E) Ab, and probed the blot with streptavidin-HRP. To confirm the specificity of the observed NIS bands, we then stripped the nitrocellulose membranes and probed them with anti-Ct-rNIS (Fig. 4C) or anti-hNIS VJ1 (Fig. 4F), thus conclusively demonstrating that Q267E NIS is targeted to the plasma membrane.

In addition, confocal immunofluorescence studies revealed a clear plasma membrane-associated immunofluorescent NIS staining pattern in COS-7 cells transfected with Q267E NIS cDNA constructs (either human or rat) (Figs 5, 6). This pattern was also indistinguishable from that observed with WT NIS. When using anti-Ct-NIS Abs, immunofluorescence was only present in permeabilized cells expressing rNIS (Fig. 5) or hNIS (Fig. 6A-D). When anti-hNIS VJ1 Ab was used (Fig. 6E-H), immunofluorescence was observed in both

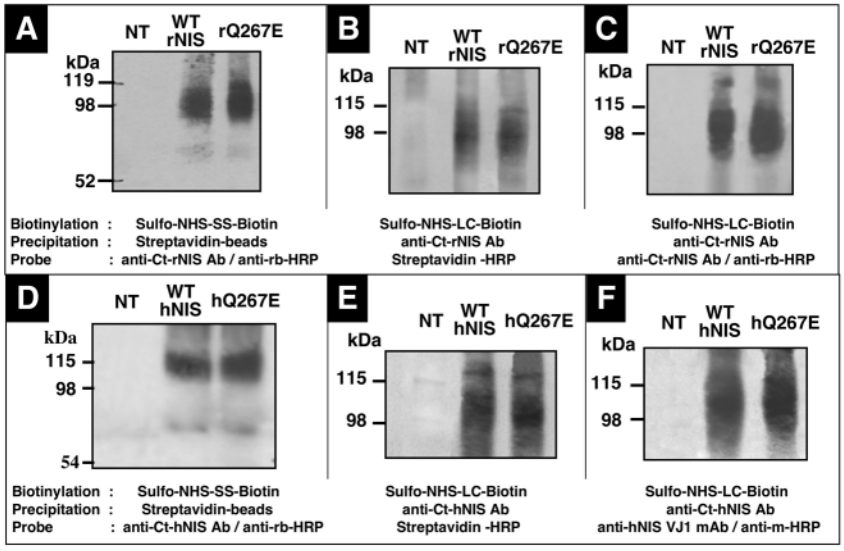

Fig. 4. Surface biotinylation analysis of Q267E NIS. Non-transfected COS-7 cells (NT) or COS-7 cells transfected with WT rNIS, rQ267E NIS, WT hNIS or hQ267E NIS were biotinylated with 1 mg/ml Sulfo-NHS-SS-biotin (A,D) or Sulfo-NHS-LC-biotin (B,C,E,F). Immunoblot analysis of surface biotinylated polypeptides precipitated with streptavidin-agarose beads was performed with either 2 nM anti-Ct-rNIS Ab (A) or 4 nM anti-Ct-hNIS Ab (D). This is a representative immunoblot. Nitrocellulose membranes were stripped and reprobed with anti-Na^+/K^+-ATPase alpha subunit antibody (not shown). Expression of both NIS and Na^+/K^+ ATPase alpha subunit was quantified in five different experiments. No statistically significant difference was found between the NIS/ATPase-alpha-subunit expression ratio of Q267E NIS and WT NIS. (B,E) Blot analysis of surface-biotinylated polypeptides immunoprecipitated with anti-Ct-rNIS (B) or anti-Ct-hNIS (E) and probed with streptavidin-HRP. (C,F) Stripped nitrocellulose membranes were reprobed with anti-Ct-rNIS (C) or anti-hNIS VJ1 (F).

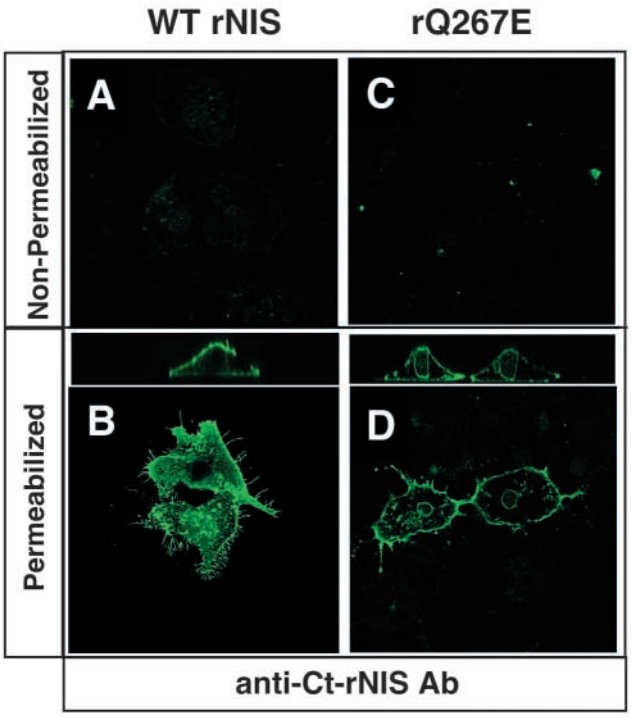

Fig. 5. Immunofluorescence analysis of COS-7 cells not transfected or transfected with WT rNIS or rQ267E NIS. Non-permeabilized (A,C) or permeabilized (B,D) transfected COS-7 cells were incubated with 2 nM anti-Ct-rNIS Ab followed by fluorescein-conjugated goat anti-rabbit Ab. The rectangular panels above B and D show *xz* cross-sectional images obtained using a confocal microscope

permeabilized and non-permeabilized cells, because of the outwardly facing epitope. These findings provide further proof that Q267E NIS is properly targeted to the cell surface.

The presence of charged residues other than glutamate at position 267 renders NIS inactive without affecting its expression or targeting to the plasma membrane

The Q267E mutation involves the presence of Glu, a residue with a negatively charged side-chain, in place of the neutral Gln. To investigate the importance of charge at position 267, we studied the effects of substituting other charged side-chains at this position. Using site-directed mutagenesis, we engineered Asp, Lys, or Arg into position 267. All constructs were transiently transfected into COS-7 cells. Transport assays showed that Q267D, Q267K and Q267R NIS mutant proteins were inactive at I^- concentrations in the range of 5-640 μM. Results obtained at 20 μM I^- are shown in Fig. 7A. Interestingly, all analyzed substitutions yielded normally expressed proteins (see western blot analysis in Fig. 7B). The levels of NIS reaching the plasma membrane were similar in all cases, as shown by cell surface biotinylation (Fig. 7C). Comparable plasma membrane-associated fluorescence was observed in cells expressing each of the NIS mutants (Fig. 7D). Clearly, all Q267 NIS mutants studied were normally expressed and properly targeted to the plasma membrane, regardless of which charged side-chain was engineered into the transporter molecule. Therefore, the effect of all three

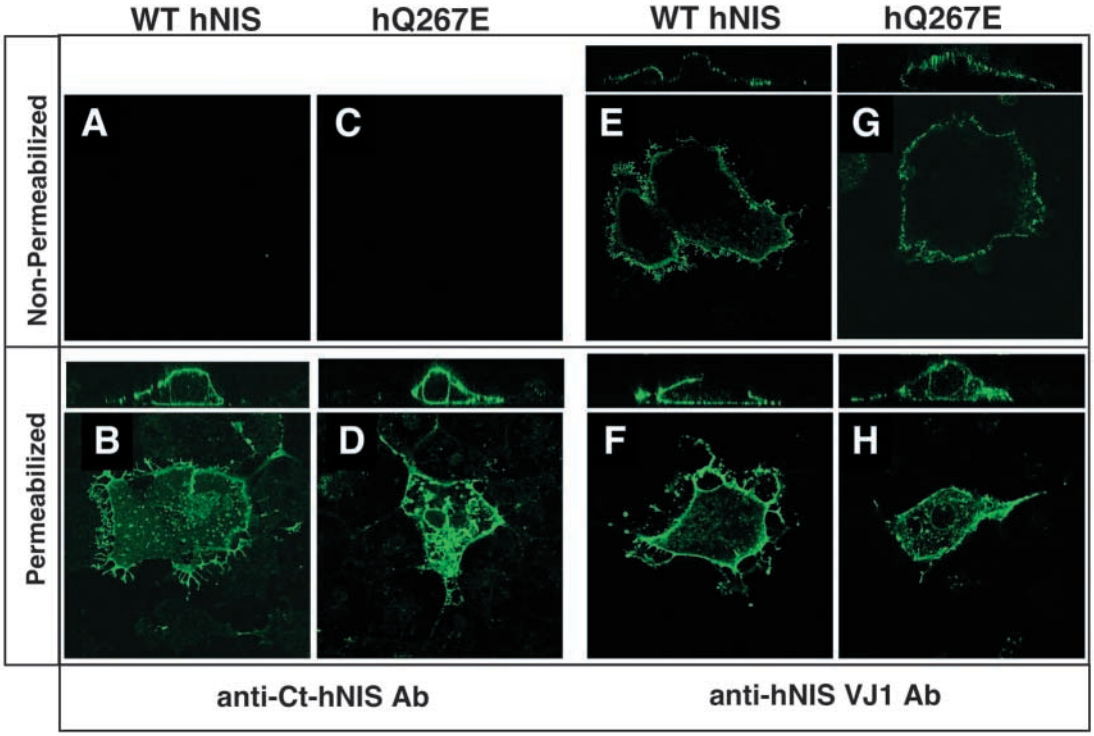

Fig. 6. Immunofluorescence analysis of COS-7 cells transfected with WT hNIS or hQ267E NIS. Non-permeabilized (top panels) or permeabilized (bottom panels) transfected COS-7 cells were incubated with 4 nM anti-Ct-hNIS Ab (A-D) or with anti-hNIS VJ1 Ab (1:50) (E-H). A second incubation was performed with fluorescein-conjugated goat anti-rabbit Ab (A-D) or fluorescein-conjugated anti-mouse Ab (E-H). The upper rectangular panels show *xz* cross-sectional images obtained using a confocal microscope.

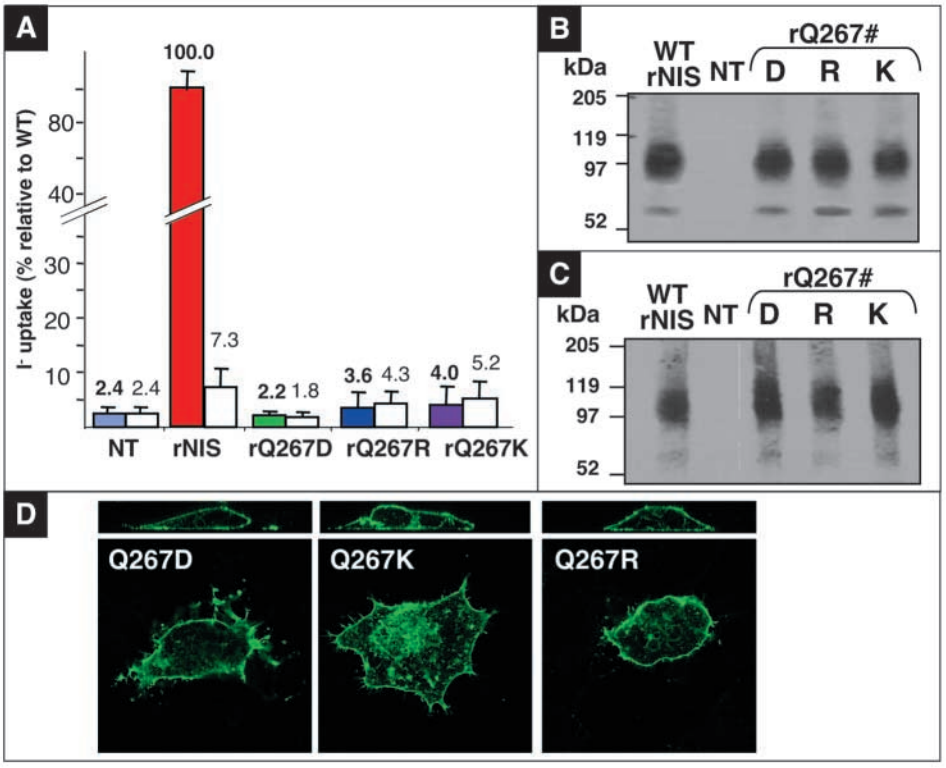

Fig. 7. Effect of charged side-chain Q267 substitutions on NIS expression. (A) Non-transfected COS-7 cells (NT) or COS-7 cells transfected with either WT rNIS or rQ267D, rQ267K or rQ267R NIS were assayed for I^- transport activity at 20 μM I^- at steady-state. Assays were performed in the presence of 20 μM I^-/140 mM Na^+ (colored bars) or 20 μM I^-/140 mM Na^+ plus 80 μM perchlorate (white bars). Results are expressed as a percentage of WT NIS activity. The *y*-axis has been split into two scales. (B) Immunoblot. (C) Surface biotinylation. (D) Immunofluorescence analysis. Procedures were performed as described in Figs 3, 5 and 6, and in Materials and Methods.

substitutions was to render NIS inactive without altering NIS expression or trafficking.

The presence of a neutral side-chain at position 267 is compatible with partial NIS activity without affecting NIS expression or targeting to the plasma membrane

To study the effects of neutral side-chain amino acid substitutions at position 267 on NIS expression, activity and targeting to the plasma membrane, we engineered the following residues into this position: Asn (an uncharged and polar residue, similar to the original glutamine, except with one fewer methylene group); Ala (an aliphatic, non-polar and α-helix-stabilizing residue); Pro (an aliphatic, non-polar and α-helix-destabilizing residue); and Trp (an aliphatic and non-polar residue with a large side-chain). I^- uptake was analyzed under steady-state conditions. At an external I^- concentration of 20 μM, Q267N and Q267A NIS exhibited I^- accumulation values of 29.5±7.5% and 18.7±3.9%, respectively, relative to WT NIS (Fig. 8A). Similar results were obtained at a saturating I^- concentration (i.e., 160 μM; Fig. 8B); I^- was accumulated by Q267N and Q267A NIS (28.3±7.6%, 22.8±7.5, relative to WT NIS). Also, modest I^- accumulation (lower than in the Glu substitution, however) was barely detected in cells expressing Q267P or Q267W NIS (data not shown). As in the charged side-chain 267 NIS amino acid substitutions, all neutral replacements yielded normally expressed (Fig. 8C) and properly targeted proteins, as shown by both surface biotinylation (Fig. 8D) and confocal immunofluorescence analyses (Fig. 8E).

Q267A, Q267N and Q267E NIS all exhibit decreased V_{max} values for I^- as compared to WT NIS

Fig. 9A shows the kinetic properties of I^- uptake in COS-7 cells expressing Q267A, Q267N, Q267E or WT NIS. Initial rates were estimated by measuring I^- accumulation at 4 minutes over a range of I^- concentrations (2.5-200 μM). In all cases, transport showed typical Michaelis-Menten kinetics. No significant variations in the affinity for I^-, as indicated by K_m values, were observed among cells expressing the mutant proteins with respect to WT NIS (Table 1). The maximal rate of I^- uptake (V_{max}) was diminished in all mutants relative to WT NIS (Table 1). Given that Q267A, Q267N and Q267E NIS were all normally expressed (Fig. 8C) and properly targeted to the plasma membrane (Fig. 8D,E), these kinetic findings suggest that these mutations cause a reduction in the transporter turnover number.

Q267A and Q267N NIS exhibit lower V_{max} for I^- uptake as a function of the extracellular Na^+ concentration, further supporting the notion of lower turnover numbers for these mutants as compared to WT NIS

We then studied the kinetic properties of I^- uptake as a function of increasing concentrations of extracellular Na^+ in COS-7 cells expressing Q267A, Q267N, Q267E and WT NIS (Fig. 9B). The initial rate of transport was estimated by measurement of I^- accumulation after 4 minutes over a range of Na+

Table 1. Kinetic parameters

	I^-		Na^+	
	V_{max}±s.e.m.	K_m±s.e.m. (μM)	V_{max}±s.e.m.	K_m±s.e.m. (mM)
rNIS	67.4±2.1	34.8±2.8	23.8±3.8	71.9±1.7
rQ267E	6.5±0.5	70.5±11.7	2.7±1.0	67.0±6.3
rQ267A	11.0±0.5	46.6±4.6	4.0±0.7	61.7±4.4
rQ267N	13.3±0.5	40.5±3.9	4.8±0.5	59.2±4.8

Results from 5, for iodide (I^-) dependence and 3, for sodium (Na^+) dependence, kinetic experiments were adjusted to compensate for the transfection efficiency and analyzed as described in Materials and Methods. K_m and V_{max} values are expressed as mean±s.e.m.

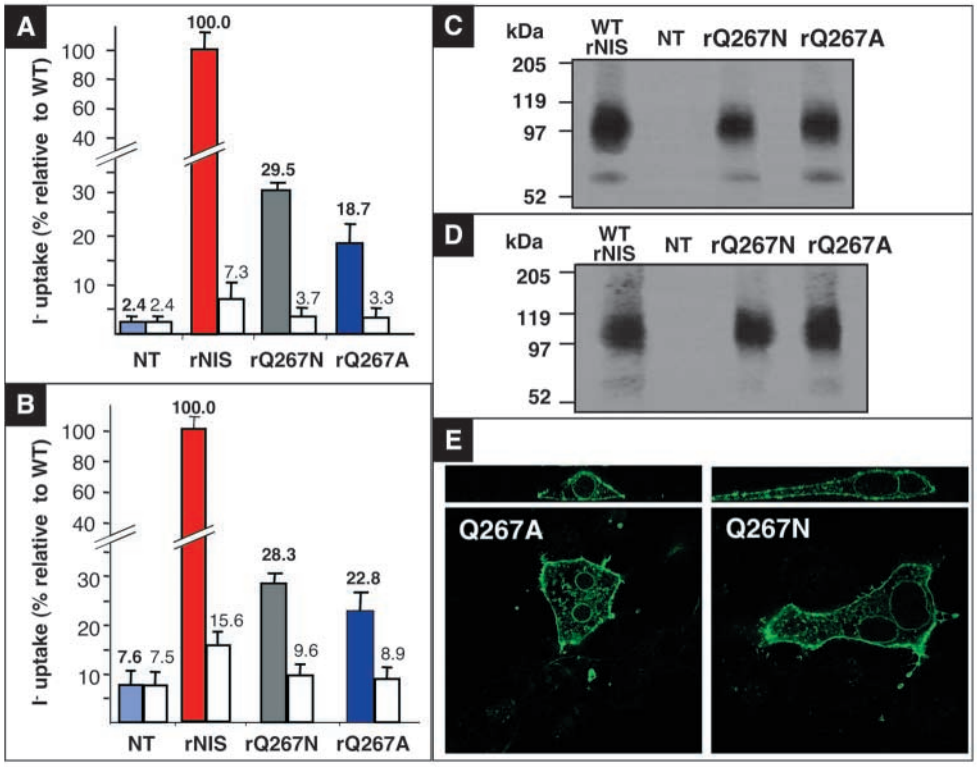

Fig. 8. Effect of neutral and polar side-chain Q267 substitutions on NIS expression. Non-transfected COS-7 cells (NT) or COS-7 cells transfected either with WT rNIS, rQ267A or rQ267N NIS were assayed for I^- transport activity at 20 (A) or 160 (B) μM I^-. Assays were performed in the presence of 20 μM or 160 μM I^-/140 mM Na^+ (colored bars) or 20 μM or 160 μM I^-/140 mM Na^+ plus 80 μM perchlorate (white bars). Results are expressed in percentages with respect to WT NIS activity. *y*-Axis has been split into two scales. (C) Immunoblot. (D) Surface biotinylation. (E) Immunofluorescence analysis. All procedures were performed as described in Figs 3, 5 and 6, and in Materials and Methods.

concentrations (0-200 mM) and at 20 μM I^-. All NIS proteins exhibited saturating I^- transport activity with typical sigmoidal Na^+ dependence, with no significant change in their affinity for Na^+ as compared to WT NIS. However, the rate of transport activity (i.e., V_{max} for Na^+) was diminished in cells expressing Q267A and Q267N NIS (Table 1). This finding is compatible with a decrease in turnover numbers for these mutants.

Discussion

We present a thorough analysis of the Q267E mutation of NIS. The identification and characterization of NIS mutations that occur naturally in patients with ITD is undoubtedly a valuable approach to study the mechanism of NIS activity and NIS structure/function relations. According to our current NIS secondary structure model (Fig. 1A), two of the ITD-causing NIS mutations are located in intracellular loops (Q267E, C272X), one in an external hydrophilic loop (fS-515X), and six within transmembrane segments (V59E, G93R, T354P, G395R, Y531X, G543E). There is also one deletion between TMS III to IX (ΔM143-Q323). The Q267E NIS mutation decreases (but does not abolish) I^- transport activity by lowering the turnover number of the molecule, without affecting NIS expression or trafficking to the plasma membrane, and without altering the affinity of NIS for I^- or Na^+. Moreover, our findings conflict with two previous studies of the Q267E NIS mutation, by Pohlenz et al. (Pohlenz et al., 1998; Pohlenz et al., 2000), who concluded that Q267E NIS was not functional and that its lack of function was due to impaired targeting of the transporter to the plasma membrane.

Our evidence is abundant. First, we showed by immunohistochemistry that NIS is overexpressed in thyroid sections from a patient with the Q267E NIS mutation (Fig. 1D,E). NIS staining was present both intracellularly and at the plasma membrane, a finding compatible with the possibility that Q267E NIS might be reaching the cell surface. Considering that the patient has long been receiving thyroid hormone treatment, the observation that NIS is overexpressed in the patient's thyroid is surprising. A possible explanation is that the patient may have been noncompliant with her substitutive hormonal treatment, as suggested by several elevated serum TSH values that have been recorded over an 11-year follow-up period (Pohlenz et al., 1998).

Second, we observed that the Q267E NIS mutant protein is normally expressed and, most importantly, exhibits modest activity in COS-7 cells transfected with Q267E NIS cDNA rat and human constructs (Fig. 2). Whereas the observed activity of Q267E NIS was admittedly much lower than that of WT NIS, the activity of Q267E NIS was clearly not entirely abolished. Indeed, Q267E NIS activity exhibited a statistically significant 2.5-fold increase over the level recorded in control non-transfected cells. Moreover, we showed that the difference in accumulation between cells expressing WT NIS and those expressing Q267E NIS decreased at higher substrate concentrations. The demonstration of any level of significant NIS activity in Q267E-NIS-expressing cells constitutes unequivocal proof that at least some Q267E NIS molecules do reach the plasma membrane. Tellingly, the ~2.5 saliva/plasma (S/P) I^- ratio originally reported for the patient bearing the Q267E NIS mutation (Pohlenz et al., 1998) reflects the 2.5-fold transport rate measured in Q267E-NIS-expressing COS-7 cells with respect to non-transfected cells. This suggests that ~2.5-fold was approximately the level range of NIS activity in the patient in vivo. By comparison, the (S/P) I^- ratios are much lower (~1) in patients bearing either the T354P or G395R NIS mutations (Fujiwara et al., 1997; Matsuda and Kosugi, 1997; Fujiwara et al., 1998; Kosugi et al., 1998a; Kosugi et al., 1999), an observation consistent with the total absence of NIS activity detected in COS-7 cells transfected with cDNA constructs for these mutants.

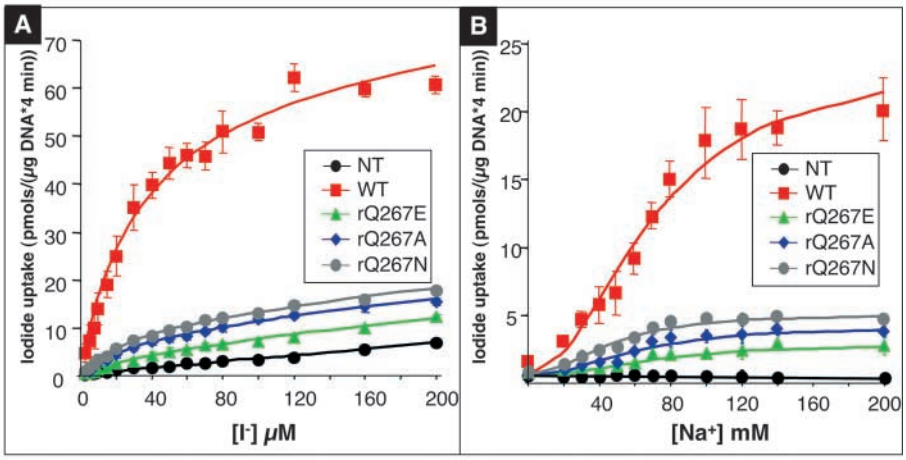

Fig. 9. Kinetic analysis of I^- uptake in transfected COS cells. (A) Initial rates (4-minute time points) of I^- uptake were determined at the indicated concentrations of I^-, as described in Materials and Methods. Calculated curves (smooth lines) were generated using the equation: $v([I^-])=(V_{max}\times[I^-])/(K_m+[I^-])+0.03\times I^-]+0.37$. The terms $0.03\times[I^-]+0.37$ correspond to background adjusted by least squares to the data obtained with non-transfected cells. V_{max}-I^- and K_m-I^- values are indicated in Table 1. Symbols: non-transfected cells (black circles), WT NIS (red squares), rQ267E (green triangles), rQ267A (blue diamonds) and rQ267N (gray circles). (B) Na^+-dependent kinetic analysis. To assess Na^+ dependence of I^- uptake, cells were incubated for 4 minutes with the indicated concentrations of Na^+; isotonicity was maintained constant with choline chloride. Na^+ dependence data were analyzed using the equation $v=(V_{max}\times[Na^+]^2)/(K_m+[Na^+]^2)-0.001\times[Na^+]+0.87$. The term $0.001\times[Na^+]+0.87$ corresponds to the background adjusted by lineal regression analysis obtained with non-transfected cells. Data were fitted by non-linear least squares using the Marquard-Levenberg algorithm (Press et al., 1986). V_{max}-Na^+ and K_m-Na^+ values are indicated in Table 1.

The discrepancy between our findings and those of Pohlenz et al. (Pohlenz et al., 1998; Pohlenz et al., 2000) may be the result of differences in transfection efficiency. We observed that when the transfection efficiency was lower than 10%, as assessed by flow cytometry, no significant differences of I^- accumulation were observed between Q267E NIS-expressing COS-7 cells, non-transfected cells, or cells transfected with the empty vector only. Therefore, as Q267E NIS is considerably less active than WT NIS, the transfection efficiency is critical to detect activity. It is possible that the transfection efficiency in the studies by Pohlenz et al. (Pohlenz et al., 1998; Pohlenz et al., 2000) may have been below the 10% threshold.

Third, we conclusively demonstrated that targeting of Q267E NIS to the plasma membrane is indistinguishable from that of WT NIS by flow cytometry, surface biotinylation and confocal immunofluorescence (Figs 3-6). Analysis by flow cytometry revealed Q267E NIS in the plasma membrane by the use of either the anti-carboxyl terminus NIS Ab, which is directed against an intracellularly oriented epitope, or the monoclonal anti-hNIS VJ1 Ab, directed against an extracellularly oriented epitope (Fig. 3). A similar percentage of cells expressing Q267E or WT NIS was detected by flow cytometry with either antibody (Fig. 3), thus showing no quantitative trafficking differences between both proteins. Similar immunofluorescence and flow cytometry results were observed when flag-rNIS and flag-rQ267E constructs were transfected in COS-7 cells (data not shown). Surface biotinylation studies also revealed similar levels of Q267E and WT NIS at the plasma membrane (Fig. 4). Both the immunoblot analysis showing the same degree of expression of mutant and WT NIS and the biotinylation analysis displaying similar levels of both proteins at the plasma membrane were confirmed in transiently transfected HEK-293 cells as well (data not shown).

Our confocal immunofluorescence experiments showed a clear plasma membrane-associated immunofluorescent NIS staining pattern in COS-7 cells transfected with either Q267E NIS cDNA constructs (human or rat) or WT NIS (Figs 5, 6). Plasma membrane-associated immunofluorescence observed with the use of the anti-carboxyl terminus NIS Ab may reflect either actual plasma membrane localization of the protein or localization in plasma membrane-associated organelles rather than the plasma membrane itself, given the intracellular orientation of the carboxy terminus. Hence, we also demonstrated a similar plasma membrane-associated immunofluorescent NIS staining pattern using the monoclonal anti-hNIS VJ1 Ab, which recognizes the last two extracellular loops of NIS (Pohlenz et al., 2000). This provides additional evidence supporting the conclusion that Q267E NIS is properly targeted to the cell surface. In stark contrast to all the above findings, we have observed that a different ITD-causing NIS mutation, namely G543E, actually causes NIS to be retained intracellularly (De la Vieja et al., unpublished).

To better understand the effects and structure/function implications of the Q267E mutation, we engineered several residue substitutions at position 267 by site-directed mutagenesis. We observed that the presence of virtually any charged side-chain at this position, with the important exception of Glu (i.e., the original mutation), renders NIS inactive without affecting its expression or its targeting to the plasma membrane (Fig. 7). In contrast, the presence of a neutral side-chain at position 267 is compatible with partial NIS activity, without affecting NIS expression or targeting to the plasma membrane (Fig. 8). Both at subsaturating (20 µM) and saturating (160 µM) external concentrations of I^-, NIS with Asn at position 267 accumulated ~30% and with Ala ~20% of wild-type levels. Gln (volume 143.9 $Å^3$) and Asn (volume 117,1 $Å^3$) have polar side chains that can form hydrogen bonds with the amide groups functioning as hydrogen donors and the carbonyl groups functioning as acceptors. However, Gln has one more methylene group than Asn; this allows Gln to reach further than Asn, provides the polar group more flexibility, and reduces its interaction with the main peptide chain. It is therefore not surprising that Q267N NIS is active, even though it displays lower activity than WT NIS, probably because of the existence of weaker hydrogen bonds, as the Asn side chain has a shorter reach than that of Gln. Q267A NIS activity could be explained by the possibility that the absence of one

methylene and the carboxyamide of Gln leaves enough space for a water molecule to occupy the position of the carboxyamide and partially replace the hydrogen bond donor and acceptor functions of Gln, as has been shown to occur in the case of the N105A substitution in T_4 lysozyme (Xu et al., 2001).

As protonated glutamic acid is much more similar to Gln than unprotonated glutamate, the markedly reduced activity (5.9%) of Q267E NIS may be a result of the thermodynamic cost (1-3 kcal/mol) this molecule incurs to become protonated. For its part, the complete absence of function in Q267D may be attributed to the combination of both (30%×6%=1.8%) the shorter reach and the energetic cost. The kinetic properties of Q267E NIS protein were barely measurable because of the small amount of I^- transport. Q267E NIS showed a lower apparent affinity for I^- (70.5 μM) than WT NIS did (34.8 μM); however, this lower affinity is not enough to account for the dramatic decrease in V_{max} Q267E NIS (6.5 pmol I^-/μg DNA/4 minutes) versus WT NIS (67.4 pmol I^-/μg DNA/4 minutes). In the case of Q267A and Q267N NIS, the apparent affinities for Na^+ and I^- are quite similar to those of WT NIS (Fig. 9 and Table 1). Taken together, these results suggest that Q267 must not be a part of the Na^+ and/or I^- binding sites. Therefore, the most likely explanation for the absent (Q267D,R,K,P,W) or reduced (Q267E<A<N) activity displayed by the different NIS proteins is that Q267 provides key internal hydrogen bonds that stabilize the initial or final state of a conformational change involving the intracellular hydrophilic segment that joins TMS VII and VIII.

That only 29 ITD mutations of NIS cDNA have been sequenced to date does not exclude the prospect that more mutations in the NIS molecule will be found. It is possible that other mutations only partially affect NIS function. In a normal or high I^- diet, those molecules could transport enough I^- to maintain adequate thyroid hormone levels. However, these 'moderate or mild' ITDs could be a major problem in I^--deficient areas. Knowledge obtained from the molecular analysis of ITDs should enable us to differentiate between mutations that partially (e.g., Q267E) or totally (e.g., T354P, G395R) impair NIS function: the hydroxyl group at the β-carbon of the residue at position 354 is essential for NIS function (Levy et al., 1998c), whereas the presence of a charged or large side-chain at position 395 interferes with NIS function (Dohan et al., 2002).

In summary, Q267E NIS is correctly targeted to the plasma membrane. Initial-rate and steady-state analysis of I^- transport activity showed that Q267E NIS is active, but only concentrates I^- by a factor of ~2.5. The molecular analysis of different residue substitutions at position 267 suggests that the presence of the carboxyamide group and the size of the side-chain are important for NIS function. The structural effects of the Q267E mutation result in a decrease of the maximal rate of transport.

We thank Dr Sabine Costagliola for providing the anti-hNIS VJ1 antibody and Dr Samuel Refetoff for providing the pcDNA3.1-hQ267E cDNA and the thyroid tissue slides from the patient bearing the Q267E NIS mutation. We are grateful to Dr Mario Amzel for insightful comments and to the members of the Carrasco laboratory for critical reading of the manuscript. A.V. was supported in part by Ministry of Education and Culture (Ministerio de Educación y Cultura) of Spain PF 97 52094152. This project was supported by the National Institutes of Health DK-41544 (N.C.).

References

Carrasco, N. (1993). Iodide transport in the thyroid gland. *Bioch. Biophys. Acta* **1154**, 65-82.

Castro, M. R., Bergert, E. R., Beito, T. G., Roche, P. C., Ziesmer, S. C., Jhiang, S. M., Goellner, J. R. and Morris, J. C. (1999). Monoclonal antibodies against the human sodium iodide symporter: utility for immunocytochemistry of thyroid cancer *J. Endocrinol.* **163**, 495-504.

Chen, J. G., Liu-Chen, S. and Rudnick, G. (1998). Determination of External Loop Topology in the Serotonin Transporter by Site-directed Chemical Labeling. *J. Biol. Chem.* **273**, 12675-12681.

Chung, J. K. (2002). Sodium iodide symporter: its role in nuclear medicine. *J. Nucl. Med.* **43**, 1188-1200.

Dai, G., Levy, O. and Carrasco, N. (1996). Cloning and characterization of the thyroid iodide transporter. *Nature* **379**, 458-460.

De la Vieja, A., Dohan, O., Levy, O. and Carrasco, N. (2000). Molecular analysis of the sodium/iodide symporter (NIS): Impact on thyroid and extrathyroid pathophysiology. *Physiological Rev.* **80**, 1083-1105.

Dohan, O., Baloch, Z., Banrevi, Z., Livolsi, V. and Carrasco, N. (2001). Rapid communication: predominant intracellular overexpression of the Na^+/I^- symporter (NIS) in a large sampling of thyroid cancer cases. *J. Clin. Endocrinol. Metab.* **86**, 2697-2700.

Dohan, O., Gavrielides, M. V., Ginter, C., Amzel, L. M. and Carrasco, N. (2002). Na^+/I^- symporter activity requires a small and uncharged amino acid residue at position 395. *Mol. Endocrinol.* **16**, 1893-1902.

Dohan, O., de la Vieja, A., Paroder, V, Riedel, C., Artani, M., Reed, M., Ginter, C. S. and Carrasco, N. (2003). The sodium/iodide Symporter (NIS): characterization, regulation, and medical significance. *Endocr. Rev.* **24**, 48-77.

Eskandari, S., Loo, D. D. F., Dai, G., Levy, O., Wright, E. M. and Carrasco, N. (1997). Thyroid Na^+/I^- symporter: mechanism, stoichiometry, and specificity. *J. Biol. Chem.* **272**, 27230-27238.

Fujiwara, H., Tatsumi, K., Miki, K., Harada, T., Miyai, K., Taki, S. and Amino, N. (1997). Congenital hypothyroidism caused by a mutation in the Na^+/I^- symporter. *Nature Gen.* **16**, 124-125.

Fujiwara, H., Tatsumi, K., Miki, K., Harada, T., Okada, S., Nose, O., Kodama, S. and Amino, N. (1998). Recurrent T354P mutation of the Na+/I symporter in patients with iodide transport defect. *J. Clin. Endocrinol. Metab.* **83**, 2940-2943.

Jacobberger, J. W., Fogleman, D. and Lehman, J. M. (1986). Analysis of Intracellular Antigens by Flow Cytometry. *Cytometry* **7**, 356-364.

Jacobberger, J. W. (1991). Intracellular Antigen Staining: Quantitative Immunofluorescence. *Methods* **2**, 207-218.

Kosugi, S., Sato, Y., Matsuda, A., Ohyama, Y., Fujieda, K., Inomata, H., Kameya, T., Isozaki, O. and Jhiang, S. M. (1998a). High prevalence of T354P sodium/iodide symporter gene mutation in japanese patients with iodide transport defect who have heterogeneous clinical pictures. *J. Clin. Endocrinol. Metab.* **83**, 4123-4129.

Kosugi, S., Inoue, S., Matsuda, A. and Jhiang, S. M. (1998b). Novel, missense and loss-of-function mutations in the sodium/iodide symporter gene causing iodide transport defect in three Japanese patients. *J. Clin. Endocrinol. Metab.* **83**, 3373-3376.

Kosugi, S., Bhayana, S. and Dean, H. J. (1999). A novel mutation in the sodium/iodide symporter gene in the largest family with iodide transport defect. *J. Clin. Endocrinol. Metab.* **84**, 3248-3253.

Kosugi, S., Okamoto, H., Tamada, A. and Sanchez-Franco, F. (2002). A novel peculiar mutation in the sodium/iodide symporter gene in spanish siblings with iodide transport defect. *J. Clin. Endocrinol. Metab.* **87**, 3830-3836.

Levy, O., Dai, G., Riedel, C., Ginter, C. S., Paul, E. M. and Carrasco, N. (1997). Characterization of the thyroid Na^+/I^- symporter with an anti-COOH terminus antibody. *Proc. Natl. Acad. Sci. USA* **94**, 5568-5573.

Levy, O., de la Vieja, A. and Carrasco, N. (1998a). The Na^+/I^- symporter (NIS): recent advances. *J. Bioenerg. Biomem.* **30**, 195-206.

Levy, O., de la Vieja, A., Ginter, C. S., Dai, G., Riedel, C. and Carrasco, N. (1998b). N-linked glycosylation of the thyroid Na^+/I^- Symporter (NIS): Implications for its secondary structure model. *J. Biol. Chem.* **273**, 22657-22663.

Levy, O., Ginter, C. S., de la Vieja, A., Levy, D. and Carrasco, N. (1998c). Identification of a structural requirement for thyroid Na^+/I^- symporter (NIS) function from analysis of a mutation that causes human congenital hypothyroidism. *FEBS Lett.* **429**, 36-40.

Matsuda, A. and Kosugi, S. (1997). A homozygous missense mutation of the sodium/iodide symporter gene causing iodide transport defect. *J. Clin. Endocrinol. Metab.* **82**, 3966-3971.

Pohlenz, J., Medeiros-Neto, G., Gross, J. L., Silveira, S. P., Knobel, M. and Refetoff, S. (1997). Hypothyroidism in a Brazilian kindred due to iodide trapping defect caused by a homozygous mutation in the sodium/iodide symporter gene. *Biochem. Biophys. Res. Commun.* **240**, 488-491.

Pohlenz, J., Rosenthal, I. M., Weiss, R. E., Jhiang, S. M., Burant, C. and Refetoff, S. (1998). Congenital hypothyroidism due to mutations in the sodium/iodide symporter. Identification of a nonsense mutation producing a downstream cryptic 3′ splice site. *J. Clin. Invest.* **101**, 1028-1035.

Pohlenz, J., Duprez, L., Weiss, R. E., Vassart, G., Refetoff, S. and Costagliola, S. (2000). Failure of membrane targeting causes the functional defect of two mutant sodium iodide symporters. *J. Clin. Endocrinol. Metab.* **85**, 2366-2369.

Press, W. H., Flannery, B. P., Teukolsky, S. A. and Wetterling, W. T. (1986). Numerical Recipes: The Art of Scientific Computing, pp. 523-528. Cambridge, UK: Cambridge University Press.

Smanik, P. A., Liu, Q., Furminger, T. L., Ryu, K., Sing, S., Mazzaferri, E. L. and Jhiang, S. M. (1996). Cloning of the human sodium iodide symporter. *Biochem. Biophs. Res. Commun.* **226**, 339-345.

Smanik, P. A., Ryu, K.-Y., Theil, K. S., Mazzaferri, E. L. and Jhiang, S. M. (1997). Expression, exon-intron organization, and chromosome mapping of the human sodium iodide symporter. *Endocrinology* **138**, 3555–3558.

Spitzweg, C. and Morris, J. C. (2002). The sodium iodide symporter: its pathophysiological and therapeutic implications. *Clin. Endocrinol.* **57**, 559-574.

Stephenson, L. S., Latram, M. C. and Ottesen, E. A. (2000). Global malnutrition. *Parasitology* **121**, S5-S22.

Tazebay, U. H., Wapnir, I. L, Levy, O., Dohan, O., Zuckier, L. S., Zhao, Q. H., Deng, H. F., Amenta, P. S., Fineberg, S., Pestell, R. G. and Carrasco, N. (2000). The Na^+/I^- symporter (NIS) is expressed in mammary gland during lactation and in breast cancer. *Nature Medicine* **6**, 871-878.

Weiss, S. J., Philp, N. J. and Grollman, E. F. (1984). Iodide transport in a continuous line of cultured cells from the thyroid. *Endocrinology* **114**, 1090-1098.

Wolff, J. (1983). Congenital goiter with defective iodide transport. *Endocr. Rev.* **4**, 240-254.

Xu, J., Baase, W. A., Quillin, M. L., Baldwin, E. P. and Matthews, B. W. (2001). Structural and thermodynamic analaysis of the binding of solvent at internal sites in T4 lysozyme. *Protein Sci.* **10**, 1067-1078.